DIFFUSION AND ENERGY MODELLING OF AN ARGON PLASMA DISCHARGE IN A UNIFORM MAGNETIC FIELD

F. Vidal[1], **T.W. Johnston[1],** J. Margot[2], M. Chaker[1], A. Aliouchouche[1] and O. Pauna[2]

[1]*INRS-Énergie et Matériaux, C.P. 1020, Varennes, Québec J3X 1S2 CANADA*

[2]*Département de Physique, Université de Montréal, C.P. 6128, Succ. Centre-Ville, Montréal, Québec H3C 3J7 CANADA*

(enquiries to vidal@inrs-ener.uquebec.ca *or to* johnston@inrs-ener.uquebec.ca)

The usual scalar fluid equations are used for cold ions, isothermal Maxwellian electrons are used to obtain two equations. The first equation is a power balance equation involving the energy per electron and the temperature-dependent ionization rate along the lines of Glaude et al. [1]. In the form used by Lee and Lieberman [2] the power balance is here given by the power per electron: Power/Volume$<n>_V$ = Θ = $[\nu_I(\varepsilon_I+3kT_e) + \nu_{4s}\varepsilon_{4s} + \nu_{4p}\varepsilon_{4p}]$. (The last expression is for singly ionized argon and includes 4*s* and 4*p* excitation.) The second equation is for number balance ($n^{-1}\partial n/\partial t = 0$) per electron or per ion. This is the balance between the ionization rate ν_I and the diffusion loss as calculated from quasi-neutral anisotropic diffusion operator (following the discussion of Lieberman and Lichtenberg [2]) with perpendicular and parallel diffusion coefficients $D_\perp = (k/e)\mu_{\perp i}T_e$ and $D_z = D_a = (k/e)(T_e+T_i)(\mu_i^{-1}+\mu_e^{-1})$. For a given geometry this equation provides the normalised ionization rate in the form ν_I/pT_{eV} and hence indirectly the value for the temperature required. While for simple cylinder this last quantity at number balance is given by the analytic expression for diffusion loss normalised so as to be independent of the electron temperature T_{eV}, namely, $(\mu_i p)p^{-2}[(2.4048/R)^2(1+(\mu_i pB)^2p^{-2})^{-2} + (\pi/L)^2]$, the equivalent value can be obtained numerically for any given value of $\mu_i^2B^2$.

From the number balance equation one obtains the ionization rate and hence the temperature. Some typical results are shown in Fig. 1a and Fig. 1b, for ν_I/pT_{eV} and for T_{eV} (for a power of 270W at 1 mTorr and the dimensions given in the Figures). Since the single-cylinder spatial *form* for $n/<n>_V$ is independent of the magnetic field, the variation of the loss rate with magnetic field is thus given entirely by the last expression (enclosed by [,]) in the diffusion loss result. At low values for $\mu_i^2B^2$ the diffusion is isotropic, and here is almost completely radial, varying only slightly as the length is changed by a factor of two. At very high magnetic fields the diffusion is essentially axial and hence it (and hence ν_I/pT_{eV}) decreases by a factor of four as the length is doubled. From the temperature on can calculate the power per electron-ion pair Θ and then, from the total power absorbed (a quantity easily

obtained experimentally) the total number of electron-ion pairs and hence the electron density from the normalised form. For the same cases in Fig. 1, the results are given in Fig. 2a and Fig. 2b respectively for Θ and for the maximum density n_0. In Figs. 1b and Figs. 2a, 2b are also shown (circles) experimental points from an actual experiment whose two-cylinder dimensions resemble somewhat those of the simple cylinders shown.

Often plasmas of interest exist in a more complicated geometry, such as that of the two abutting coaxial cylinders, where the cylinder with the smaller diameter represents that of the exciter and the cylinder with the larger diameter is the reactor volume. Now as the magnetic field is changed, unlike the single cylinder case, the relative distribution of the plasma density changes. To understand the behaviour of the full system it proves useful to consider two related single-cylinder cases. For the behaviour at lower values for *B* the single cylinder to examine is that with the diameter of the large cylinder and its length. At the higher values for *B*, the relevant cylinder is the one with the small diameter and the total length of the whole system. To make the point clearly, an extreme two-cylinder case is shown first in Fig. 3a, with a cylinder of very small diameter (3.75 cm) and 15cm length, co-axially abutting a large cylinder with a diameter of 30 cm and a length of 30 cm. In Fig. 3a are shown the full numerical result (as before, for 1 mTorr and 270 W) as a solid line, where, in contrast to a single cylinder, a two-step result is clearly seen. Also shown are the two single-cylinder results mentioned above, 30 cm diameter with 30 cm length (long dashes) and 3.75 diameter with 45 cm length (shorter dashes). It is clear from the figure that three statements can be made. First, at the lower magnetic fields the cylinder with the larger diameter represents the behaviour quite well. Second, at the higher magnetic fields the second cylinder better represents the results. Third, the actual result for Θ (and hence the values for *n*) are always somewhat below (above) the smaller (larger) of the single-cylinder approximations. This behaviour is easily understood on referring to Fig. 3b, where density contours are shown.

At low magnetic fields the radial diffusion is so high in the small cylinder that there is little plasma there and the behaviour is well approximated by just considering the larger cylinder as if that was all that there was. This does, however, somewhat under-estimate the volume occupied by the plasma and thus slightly overestimate Θ. At the higher *B*-field values, radial diffusion becomes nearly negligible even for the narrow cylinder and the slower diffusion associated with overall length favours the plasma confined by the magnetic field within the smaller-diameter cylinder. Thus it is clear why these two single-cylinder cases are good approximations in appropriate values for the magnetic field. A somewhat more practical and less extreme case is shown in Fig. 4a, Fig. 4b, with a cylinder of moderate diameter (15 cm) and 15cm length, co-axially abutting the same large cylinder with a diameter of 30 cm

and a length of 30 cm. As before, in Fig. 4a, the appropriate single cylinders clearly limit the behaviour of the actual system, but now the two-step behaviour is no longer evident.

References

[1] V.V. Glaude, M. Moisan, R. Pantel, P. Leprince and J. Marec, J. Appl. Phys., **51**(11) 5693 (1980).

[2] C. Lee and M.A. Leiberman: J. Vac. Sci. Technol. A **13**(2) 368 (1995).

[3] M.A. Lieberman and A.J. Lichtenberg: Principles of Plasma Discharges and Material Processing, Chap. V. John Wiley, N.Y., 1994.

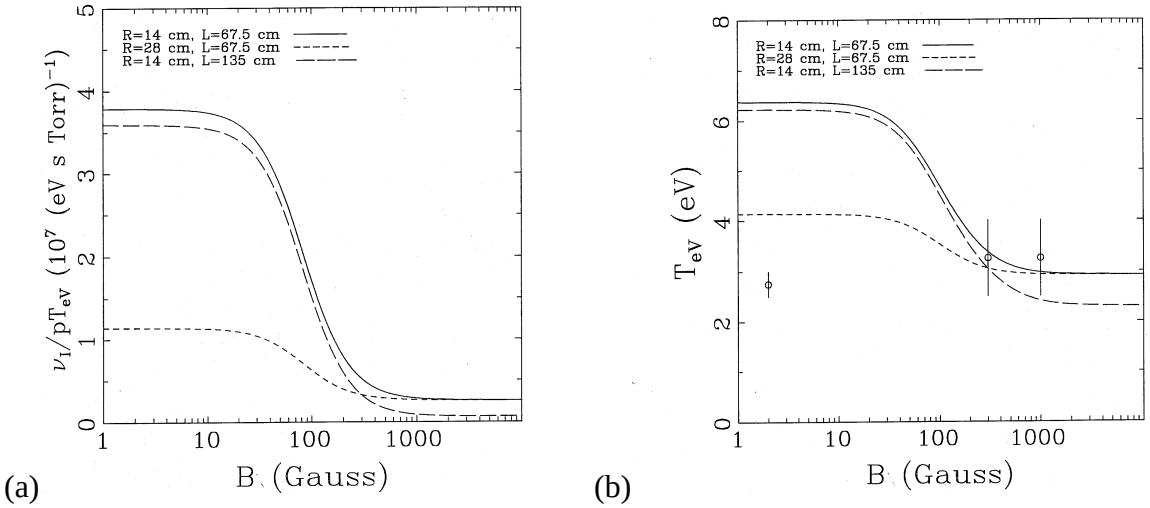

Fig. 1. Argon plasma, at 1 mTorr and 270 W, for three cylinders, effects of magnetic field *B*: (a) on ionization frequency ν_I , (b) on electron temperature T_{eV}.

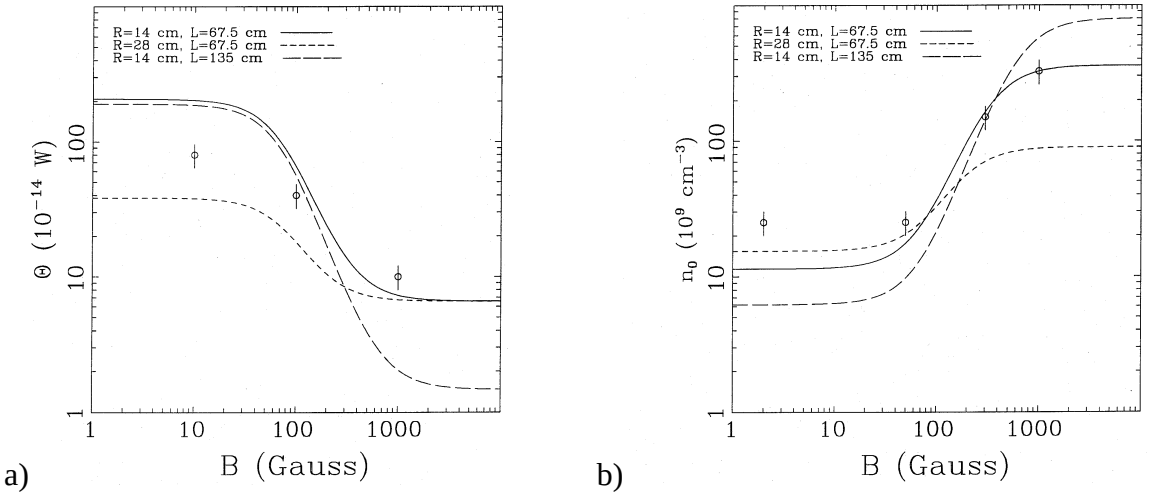

Fig. 2. Argon plasma, at 1 mTorr and 270 Watts, for three cylinders, effects of magnetic field *B*: (a) on power per electron-ion pair Θ, (b) on electron density maximum n_0.

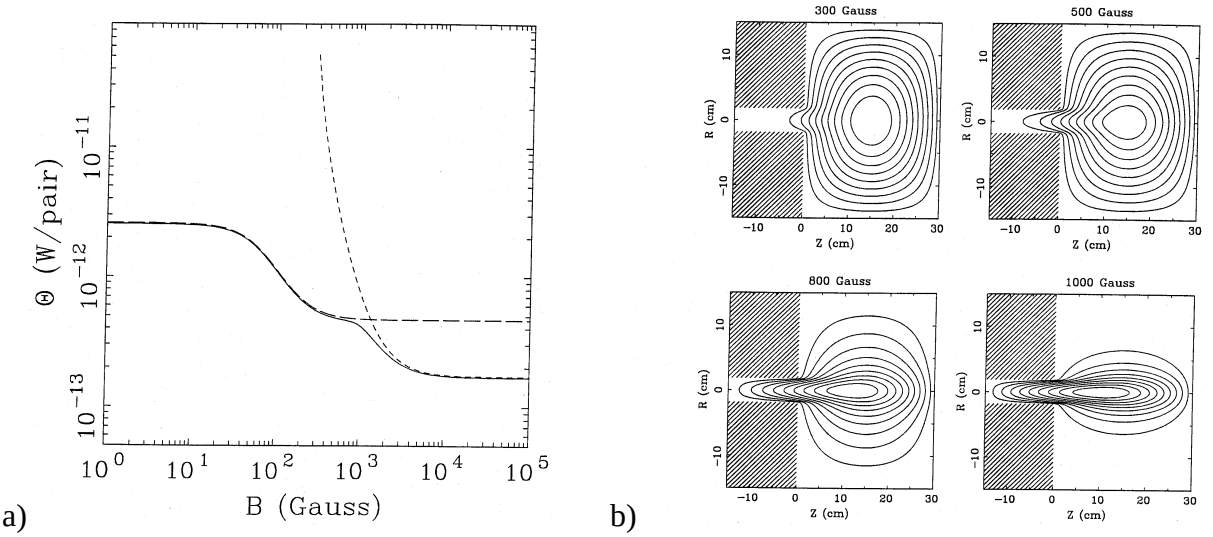

Fig. 3. Argon plasma, at 1 mTorr and 270 Watts, for an extreme combination of two co-axial abutting cylinders (3.75 cm diameter, 15 cm length and 30 cm diameter 30 cm length), effects of magnetic field *B: (a) on* Θ, (b) on electron density contours.

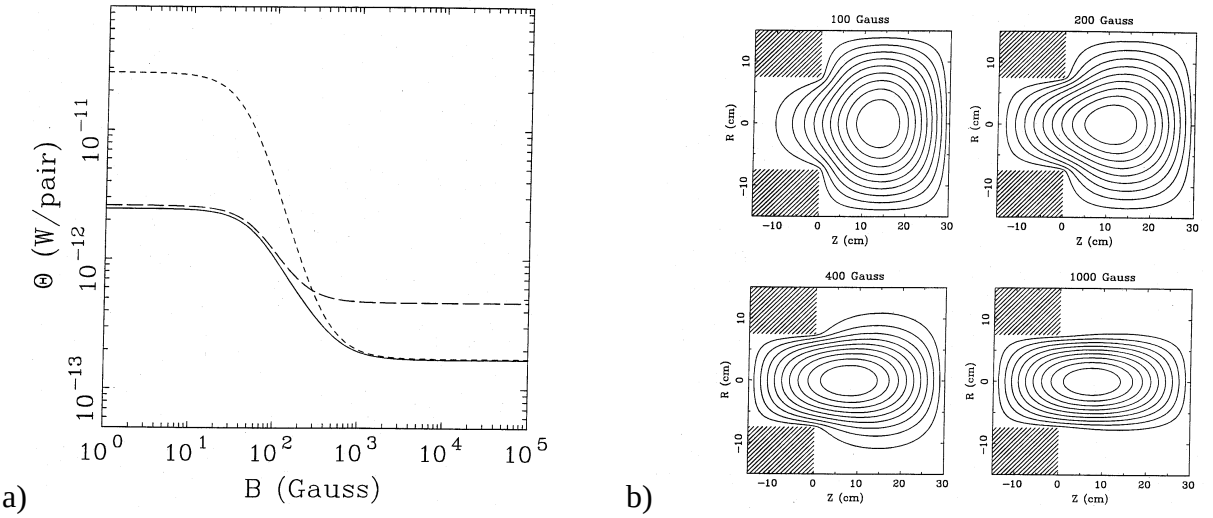

Fig. 4. Argon plasma, at 1 mTorr and 270 Watts, for a moderate combination of two co-axial abutting cylinders (15 cm diameter, 15 cm length and 30 cm diameter 30 cm length), effects of magnetic field *B*: (a) on Θ, (b) on electron density contours.